

Lawrence Berkeley National Laboratory

LBL Publications

Title

Amphiphilic Polyphosphazene for Fluorocarbon Emulsion Stabilization.

Permalink

<https://escholarship.org/uc/item/5022p8hp>

Authors

Wang, Yongkang

Liu, Wei

Zang, Zhiyi

et al.

Publication Date

2024-04-04

DOI

10.1002/sml.202312275

Copyright Information

This work is made available under the terms of a Creative Commons Attribution License, available at <https://creativecommons.org/licenses/by/4.0/>

Peer reviewed

Amphiphilic Polyphosphazene for Fluorocarbon Emulsion Stabilization

Yongkang Wang¹, Wei Liu¹, Zhiyi Zang¹, Yuzheng Luo², Shuangkun Zhang¹, Thomas P. Russell^{4,5}, Shaowei Shi^{2,3*}, and Zhanpeng Wu^{1*}*

¹ State Key Laboratory of Organic-Inorganic Composites, Beijing University of Chemical Technology, Beijing 100029, China

² State Key Laboratory of Chemical Resource Engineering, Beijing Advanced Innovation Center for Soft Matter Science and Engineering, Beijing University of Chemical Technology, Beijing, 100029, China

³ Beijing Engineering Research Center for the Synthesis and Applications of Waterborne Polymers, Beijing University of Chemical Technology, Beijing 100029, China

⁴ Department of Polymer Science and Engineering, University of Massachusetts, Amherst, Massachusetts 01003, USA

⁵ Materials Sciences Division, Lawrence Berkeley National Laboratory, 1 Cyclotron Road, Berkeley, California 94720, USA

KEYWORDS. polyphosphazene, interface, emulsion, surfactant, porous material

ABSTRACT. High internal phase emulsions (HIPEs) have been of great interest for fabricating fluorinated porous polymers having controlled pore structures with excellent physicochemical properties. However, it remains a challenge to prepare stable fluorocarbon HIPEs, due to the lack of suitable surfactants. By randomly grafting hydrophilic and fluorophilic side chains to polyphosphazene (PPZ), a comb-like amphiphilic PPZ surfactant with biodegradability was designed and synthesized for stabilizing water/fluorocarbon oil-based emulsions. The hydrophilic-lipophilic balance of PPZs can be controlled by tuning the grafting ratio of the two side chains, leading to the preparation of stable water-in-oil HIPEs and oil-in-water emulsions, and then to the production of fluorinated porous polymers and particles by polymerizing the oil phase. These fluorinated porous polymers show excellent thermal stability and, due to the hydrophobicity and porous structure, applications in the field of oil/water separation can be achieved.

Introduction

Fluorinated porous polymers have attracted much attention, due to their advantageous properties, including low-surface-energy, anti-corrosion, thermal stability and chemical resistance, arising from the very special properties of fluorine¹⁻⁴, and find applications in many fields, such as oil-water separation, water remediation⁵⁻⁷, gas adsorption⁸, tissue engineering⁹ and electrode materials^{10, 11}. One of the most feasible and efficient methods to prepare fluorinated porous polymers is the use of water-in-fluorocarbon high internal phase emulsions (HIPEs) as templates from polyHIPEs¹², where the continuous phase, consisting of fluorinated monomers, crosslinkers and fluorocarbon surfactants, is polymerized, followed by removal of the dispersed

phase and other non-polymerized materials. However, in comparison to the widely studied hydrocarbon HIPEs that can be stabilized by commercial hydrocarbon surfactants, such as span 80, sodium dodecylsulfate (SDS) and cationic cetyltrimethylammonium bromide (CTAB), it remains a challenge to achieve stable fluorocarbon HIPEs using traditional low-molecular-weight fluorocarbon surfactants as emulsifiers, though many different kinds of fluorocarbon surfactants, including cationic, anionic, non-ionic, zwitterionic and gemini surfactants, have been developed¹³⁻¹⁶.

Currently, fluorinated polymeric surfactants (FPSs), typically referring to amphiphilic polymers that consist of a hydrophilic part and a hydrophobic part that is partially or completely fluorinated, have been regarded as promising alternatives to low-molecular-weight fluorocarbon surfactants for the stabilization of HIPEs, in terms of their unique characteristics, including low critical micelle concentration, low surfactant dosage and low molecular mobility. For example, by using reversible addition fragmentation chain transfer (RAFT) polymerization¹⁷, a series of FPSs, including poly(2-dimethylamino)ethyl methacrylate-*b*-poly(hexafluorobutyl acrylate) (PDMAEMA-*b*-PHFBA)¹², (2-dimethylamino)ethylmethacrylate-*b*-poly(trifluoroethyl methacrylate) (PDMAEMA-*b*-PTFEMA)¹⁸ and poly(ethylene oxide)-*b*-poly(2,2,3,4,4,4-hexafluorobutyl methacrylate) (PEO-*b*-PHFBMA)¹⁹, have been synthesized and, when used as emulsifiers, stable fluorocarbon HIPEs and polyHIPE derivatives have been obtained. Nevertheless, the architecture of these FPSs have been limited to linear block copolymers, one of the most frequently used types for polymeric surfactants. Among the numerous architectures of polymer surfactants, including linear, grafted and star polymer chains, comb-like polymeric surfactants, where hydrophilic and hydrophobic side chains are covalently attached to a linear polymeric backbone, have attracted attention, due to their diverse structural characteristics

afforded by the two components of the backbone and side chains²⁰. Specifically, with side chains randomly grafted to the backbone, the resultant comb-like random copolymers can stabilize the liquid-liquid interface by adopting a Janus conformation, where the two types of side chains dissolve in different solvents, which promotes interfacial activity and emulsifying efficiency²¹.

Inspired by the development of FPSs and the advantages of comb-like random copolymers at the interface, we present the synthesis, characterization and application of a novel comb-like FPS based on the biocompatible, low-cost polyphosphazene (PPZ). As an organic-inorganic hybrid polymer, PPZ has an inorganic backbone of alternating phosphorus and nitrogen atoms, with organic side groups grafted to the phosphorus. Due to the easy tunability of functionality through the diverse chemistry of the side groups, comb-like amphiphilic PPZ can be achieved by randomly grafting hydrophobic and hydrophilic side chains, i.e., 2-(2-Methoxyethoxy)ethanol (MEEP) and octafluoropentanol (OTFP), to the backbone (Figure 1). By varying the mass ratio of MEEP and OTFP, the hydrophilic-lipophilic balance of amphiphilic PPZ at the interface can be effectively adjusted, leading to the stabilization of different types of emulsions including HIPEs and traditional emulsions. With emulsions as templates, fluorinated porous polymers and polymeric particles can be successfully prepared, showing considerable potential in the field of oil-water separation.

Results and Discussion

An amphiphilic PPZ, with MEEP as the water-soluble side group, and OTFP as the oil-soluble group, was synthesized in three steps: first, methoxyethoxy ethanol and octafluoropentanol were transformed into sodium 2(2-methoxyethoxy) ethoxide and sodium octafluoropentanol (Scheme S1). Second, linear polydichlorophosphazene (PDCP) was obtained by the polymerization of

hexachlorocyclotriphosphazene in sealed Pyrex tubes at 250 °C following a previously described method.²² The ³¹P-NMR spectrum of PDCP shows a characteristic peak at -18 ppm (Figure S1), consistent with the reported data.^{23, 24} Finally, the PDCP reacted with the mixture of sodium MEEP and sodium OTFP, yielding amphiphilic PPZ with complete replacement of the chlorine atoms (no peak at -18 ppm is seen, Figure 1b). The ³¹P-NMR and ¹H-NMR spectra of the pure MEEP (PMEEP) or OTFP substituted PPZ (POTFP) are shown in Figure S2 and used as reference data. For the co-substituted PPZ (P1 ~ P5), the grafting ratio of side group is determined by integration of the ¹H-NMR spectra, calculated by comparing the area under peak of the -CF₂H peak (6.10 ppm) and -OCH₃ peak (3.67 ppm), as shown in Figure 1c and Table 1. The weight average molecular weight (M_w) and polydispersity index (PDI) of amphiphilic PPZ are shown in Figure 1d and Table 1. The glass transition temperature (T_g) measured by differential scanning calorimetry (DSC) shows that, with the increasing MEEP content, the T_g decreases from -61 to -77 °C (Figure S3), indicating the MEEP segment is more flexible in comparison to OTFP²⁵. Thermogravimetric analysis shows that the amphiphilic PPZs have good thermal stability (Tonset: 252 - 289 °C, Figure S4 and Table S1), much better than that of other reported fluoro-surfactants (Tonset: 165 - 176.7 °C)²⁶⁻²⁸. Moreover, the degradability experiment was performed by placing P3 into 37 °C water environment (Figure 1e and Figure S5). It shows that the M_w of the P3 decreases from 320000 to 3000 g/mol within 5 months, indicating that the amphiphilic PPZ is a degradable macromolecular surfactant. The degradation mechanism, provided in Figure S6, shows that the side chains degrade first, followed by the degradation of the main chain^{29, 30}.

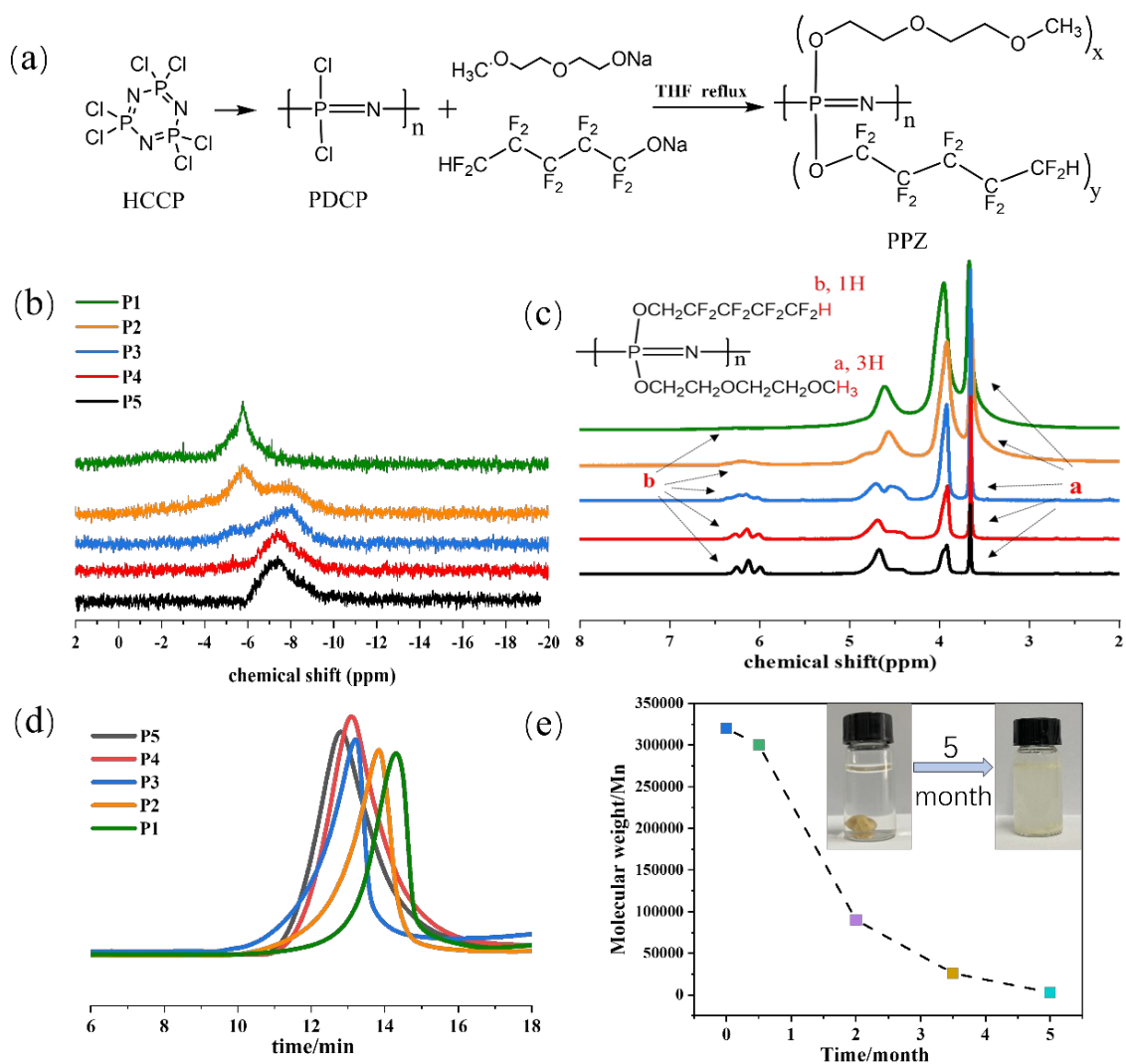


Figure 1. (a) Synthesis route of amphiphilic PPZ. (b) ^{31}P -NMR of amphiphilic PPZ and (c) ^1H -NMR of amphiphilic PPZ. (d) GPC of amphiphilic PPZ. (e) Hydrolysis of amphiphilic PPZ (P3) in water.

Table 1. Amphiphilic PPZ molecular structure and basic properties

| Sample | MEEP ^a | OTFP ^b | M_n^c | M_w^c | PDI ^c | T _g | HLB ^d |
|--------|-------------------|-------------------|---------|---------|------------------|----------------|------------------|
| P1 | 11% | 89% | 530000 | 630000 | 1.34 | -61°C | 1.2 |
| P2 | 34% | 66% | 460000 | 690000 | 1.41 | -64°C | 4.2 |
| P3 | 52% | 48% | 420000 | 560000 | 1.53 | -66°C | 7.2 |
| P4 | 73% | 23% | 350000 | 540000 | 1.59 | -68°C | 11.6 |
| P5 | 91% | 9% | 290000 | 550000 | 1.61 | -76°C | 16.8 |

a: Represents the molar proportion of hydrophilic side group diethylene glycol monomethyl ether calculated by NMR

b: Represents the molar proportion of Proportion of hydrophobic side group octafluoropentoxyl

c: Molecular weight and molecular weight distribution are characterized by GPC

d: Hydrophile-lipophile balance (HLB) represents hydrophilic–lipophilic balance, $HLB = 20 \times w_h/w$; w_h : mass of hydrophilic portion; w : mass of whole polymer; 20 is an arbitrary scaling factor^{31, 32}

The interfacial activity of the substituted PPZ graft polymers were investigated at the fluoro-oil (F-oil)/water interface, where trifluoroethyl methacrylate is used as the F-oil. As shown in Figure 2a, with POTFP dissolved in the F-oil against pure water, only a weak interfacial activity is observed, with an equilibrium interfacial tension of ~ 25 mN/m, close to that of the pure F-oil/water system (~ 27 mN/m). However, with PMEEP dissolved in the F-oil against pure water, a significant reduction in the interfacial tension from ~ 27 to ~ 8 mN/m is observed, indicating that PMEEP acts as a surfactant and can assemble at the F-oil/water interface, due to the hydrophilic MEEP segments and hydrophobic PPZ main chain. The time dependence of the interfacial tension of the co-substituted PPZ (P1~P5) is shown in Figure 2b. As the concentration of MEEP side groups increases, a gradual reduction in the interfacial tension from 22 to 2.5 mN/

m is obtained, indicating that the interfacial activity of PPZ can be adjusted by controlling the grafting ratio of MEEP and OTFP.

The logarithmic representation of the interfacial tension in Figure 2c suggests three different regimes of the assembly of amphiphilic PPZ. Using the time dependence of the interfacial tension of a 0.01 mg mL⁻¹ solution of P3 against water shown in Figure 2e as an example, three regimes in the time-dependent reduction of the interfacial tension are evident. In regime I, the interfacial tension does not decrease significantly, even though there is more than sufficient time for the amphiphilic PPZ to diffuse to the interface. This suggests that, the adsorption process of amphiphilic PPZ is very fast and has been completed once the interface is generated. In regime II, a reconfiguration of the amphiphilic PPZ at the interface occurs, where the MEEP and OTFP side chains prefer to dissolve in their good solvents. Consequently, a rapid decrease in the interfacial tension is observed. Then, in regime III, the interfacial tension remains unchanged, indicating that, for this concentration the equilibrium interfacial tension was achieved. When the concentration is increased to 0.05 mg mL⁻¹, the interfacial tension decreases slightly in regime I, similar with the case with lower concentration, and then in regime II, a rapid reduction in the interfacial tension to a much lower value is observed, due to the increased adsorption due to the higher concentration. However, in regime III, different with the case with lower concentration, the interfacial tension decreases further, indicating re-organizing of the already adsorbed chains to accommodate more PPZ. Since the re-organization at the interface is a cooperative event with other adsorbed chains, this is a slower process. When the concentration is increased to 0.1 or 0.5 mg mL⁻¹, the interfacial tension has decreased significantly, before the first measurements can be made, indicating a very rapid adsorption due to the higher concentrations. Subsequently, the interfacial tension is seen to gradually decrease, in keeping

with a re-organization of the adsorbed chains with further adsorption to reduce the interfacial tension further. From Figure 2c and 2d, it can also be seen that at a low concentration (0.01mg mL^{-1}), the interfacial tension of the F-oil/water with P5 is higher than that of P3, while at a high concentration ($\geq 0.05\text{mg mL}^{-1}$), the interfacial tension of P5 is lower than that of P3. At a low concentration, the number of either P3 or P5 assembling at the interface is very low. In comparison to P5, P3 exhibits a stronger ability to reduce the interfacial tension due to its higher amphiphilicity, forming an extended Janus conformation at the interface and, therefore, a lower surface tension is obtained. However, at a high concentration, as shown in Figure 2e, although the ability of individual P5 to reduce the interfacial tension is low, the number of P5 assembling at the interface is much higher than that of P3, since P5 has a more flexible structure and, therefore, smaller coil size. As a result, a significant reduction in the interfacial tension is observed. The change in the coil size of P1-P5 can be estimated from simulations at ambient temperature and pressure. As shown in Figure 3, with more MEEP side chains grafted to the main chain, the mean square radius of gyration of the polymer is smaller, indicating that the flexibility of MEEP plays a key role in determining the coil size of polymer. We note that the simulations were not performed in a biphasic system, but used to provide a qualitative description of the variation of polymer conformation, and this conformation must reconfigure prior to adsorption.

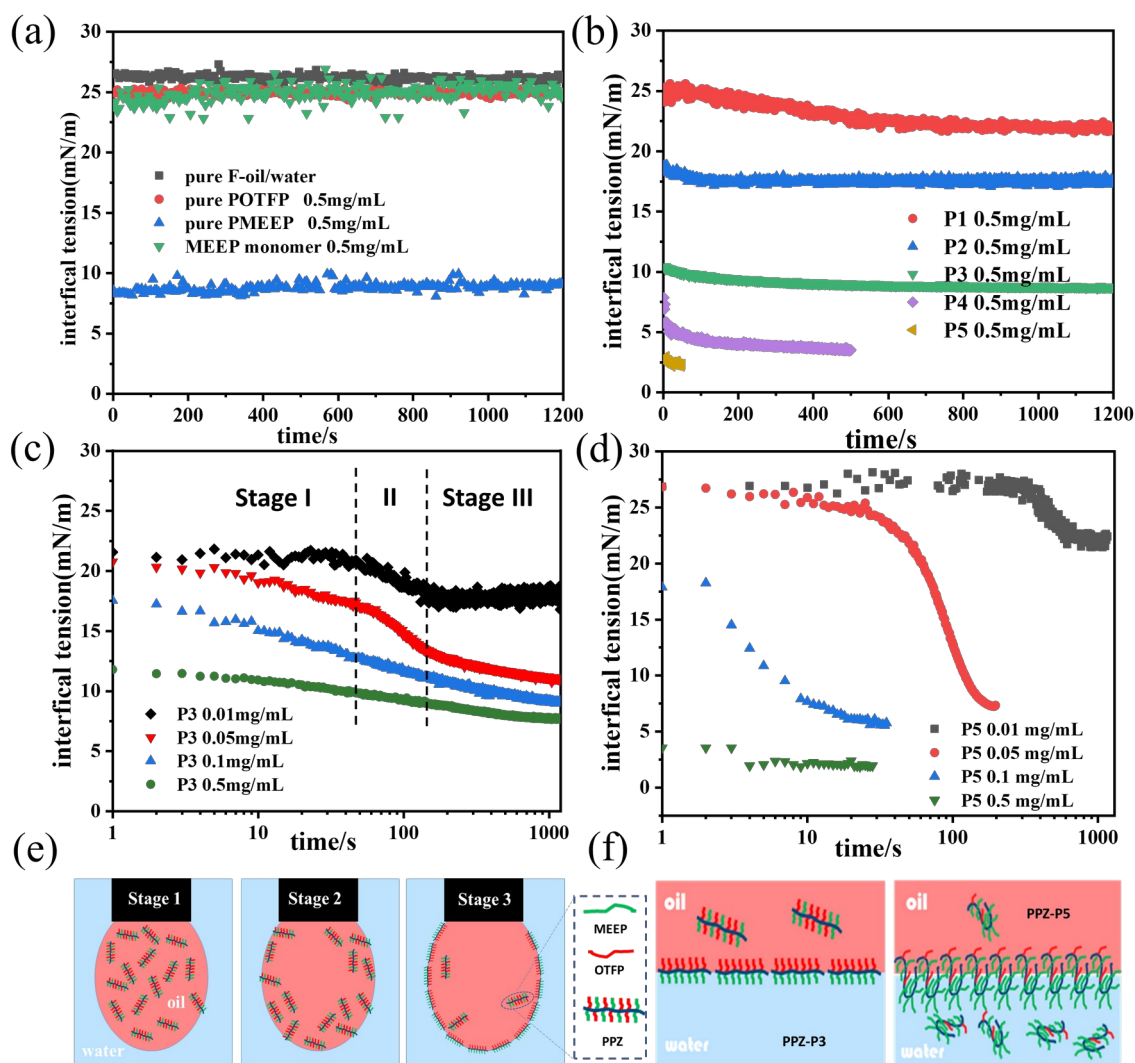


Figure 2. Regulation of PPZ on F-oil-water interfacial tension; (a) pure F-oil with water and single substituted PPZ including pure OTFP PPZ and pure MEEP PPZ and MEEP monomer, (b) co-substituted PPZ have different ratios of hydrophilicity and hydrophobicity(P1-P5). (c) effect of surfactant concentration (preferred P3) and (d) preferred P5, (e) Surfactant diffusion and interfacial assembly process, (f) conformational arrangement of amphiphilic PPZs at oil-water interface

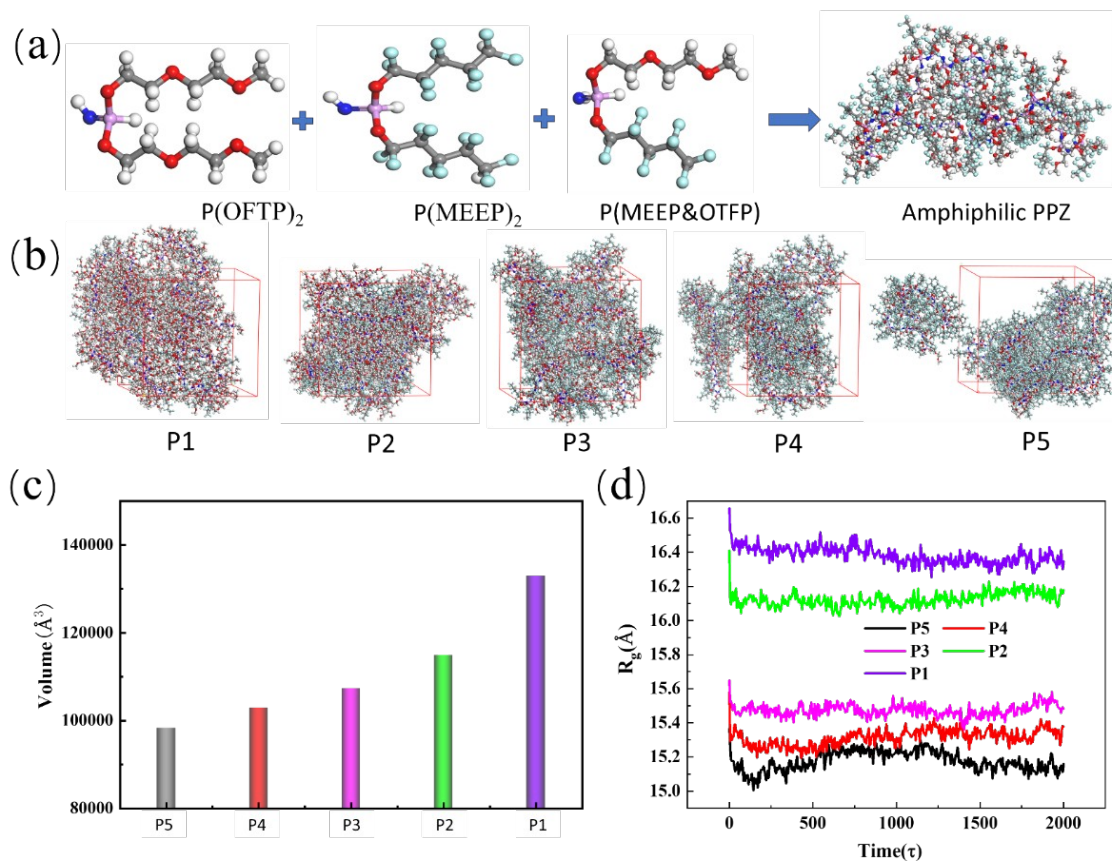


Figure 3. (a) Schematic diagram of polymer fragment simulation, (b) Polymer free volume simulation diagram, (c) polymer volume, (d) mean square radius of gyration.

Emulsions were prepared by vigorous mechanical agitation of the amphiphilic PPZ (5wt%) dissolved in F-oil with pure water. Figure 4 shows the emulsions produced by varying the molar ratio of MEEP side groups to OFTP side groups from 1/9 to 9/1, i.e., P1 to P5, at a constant 3/1 volume ratio of water and F-oil. As shown in Figure 4a-d, when using polymer P1-P4 as surfactants, water-in-F-oil (w/o) emulsions are observed. For the w/o emulsions, the drop size decreases with the increase of hydrophilic side group content (Figure 4f), from 58 to 11 μm, which is in agreement with the observed variation of the interfacial tension in Figure 2b, where the enhanced surfactancy of PPZ is beneficial for stabilizing more interface. However, with P5 as

the stabilizer, F-oil-in-water (o/w) emulsions are produced (Figure 4e). As shown in Table 1, the hydrophile-lipophile balance (HLB) for P5 is 16.8, indicating its strong hydrophilicity. As a result, the emulsion undergoes a phase transition, from a w/o emulsion to an o/w emulsion.

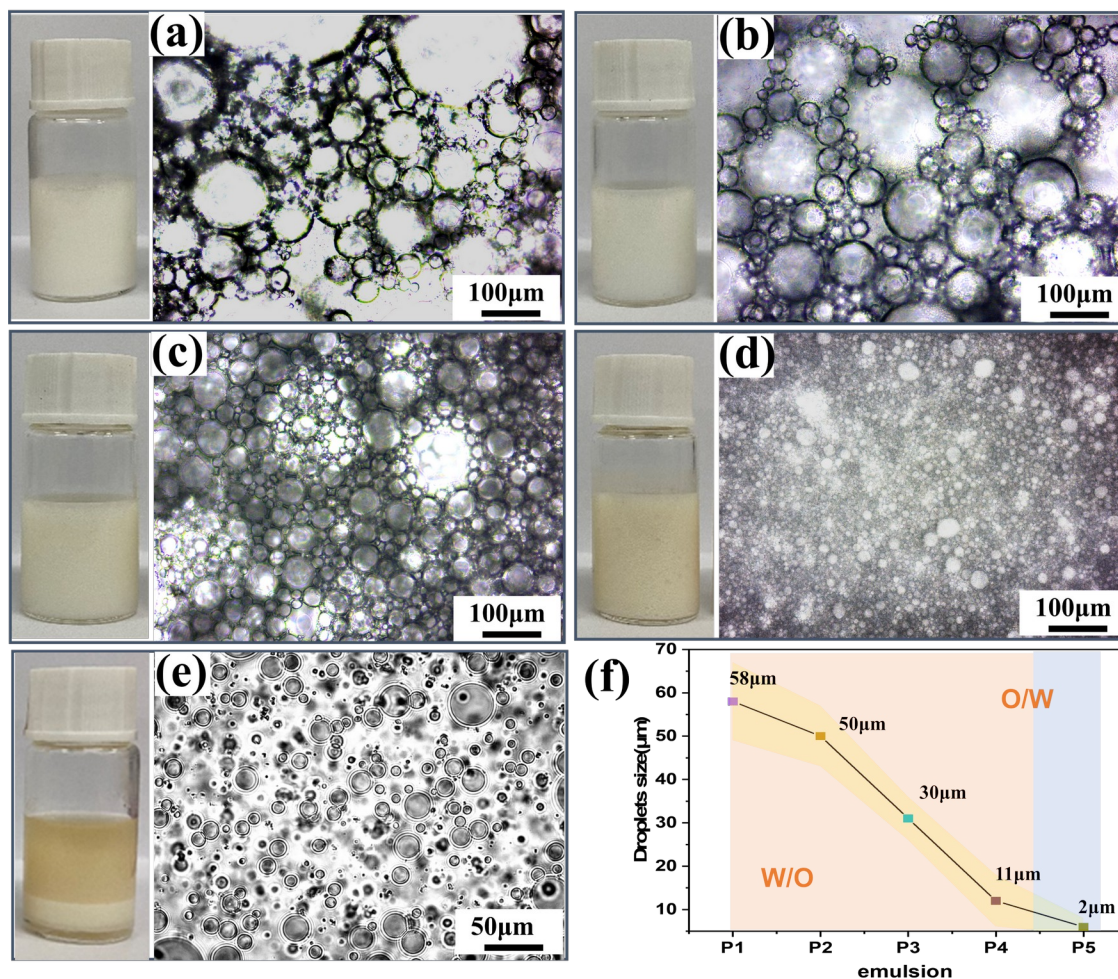


Figure 4. Visual diagram and optical microscope of fluoro-emulsion stabilized by amphiphilic polyphosphazene (5wt%) (with different hydrophobic/hydrophilic ratios, (a) P1, (b) P2, (c) P3, (d) P4, (e) P5, (f) Droplet size distribution.

Then the F-oil (TFEMA with 10wt% divinylbenzene (DVB) as crosslinker) was polymerized, resulting in a porous fluoropolymer foam or microsphere materials after removing water. For porous fluoropolymer foams, the SEM images (Figure 4a-d) show that these polyHIPEs have a homogeneous, open-cell structure with pore sizes consistent with those of the HIPE droplets (Figure 2). Fluoro-polyHIPEs with excellent mechanical strength and thermal stability can be obtained (Figure S7, Table S1), with a heat-resistant temperature > 300 °C. To a certain degree, the pore size of polyHIPE foams affects their mechanical properties. Especially for polyHIPE-P3 or polyHIPE-P4 which has a compressive strength of ~ 6.2 MPa and compressive modulus of ~ 44 MPa. This indicates that foams with smaller pore sizes have better mechanical strength, which is consistent with the results of Thomas³³. In addition, the pore size and microsphere size of the porous materials can be controlled by changing the surfactant concentration (Figure S8). The polyHIPE-P3 and polyHIPE-P4 were found to have a low thermal conductivity of 0.05 - 0.051 W m^{-1} K^{-1} , which is less than the thermal conductivity of most thermal insulation materials, such as porous beads (0.16 W m^{-1} K^{-1}), PE pipes (0.55 W m^{-1} K^{-1}), PVC pipes (0.18 W m^{-1} K^{-1}), and carbon nanotube aerogels (0.12 W m^{-1} K^{-1})^{34, 35}, indicating that this material has potential use as an insulating material.

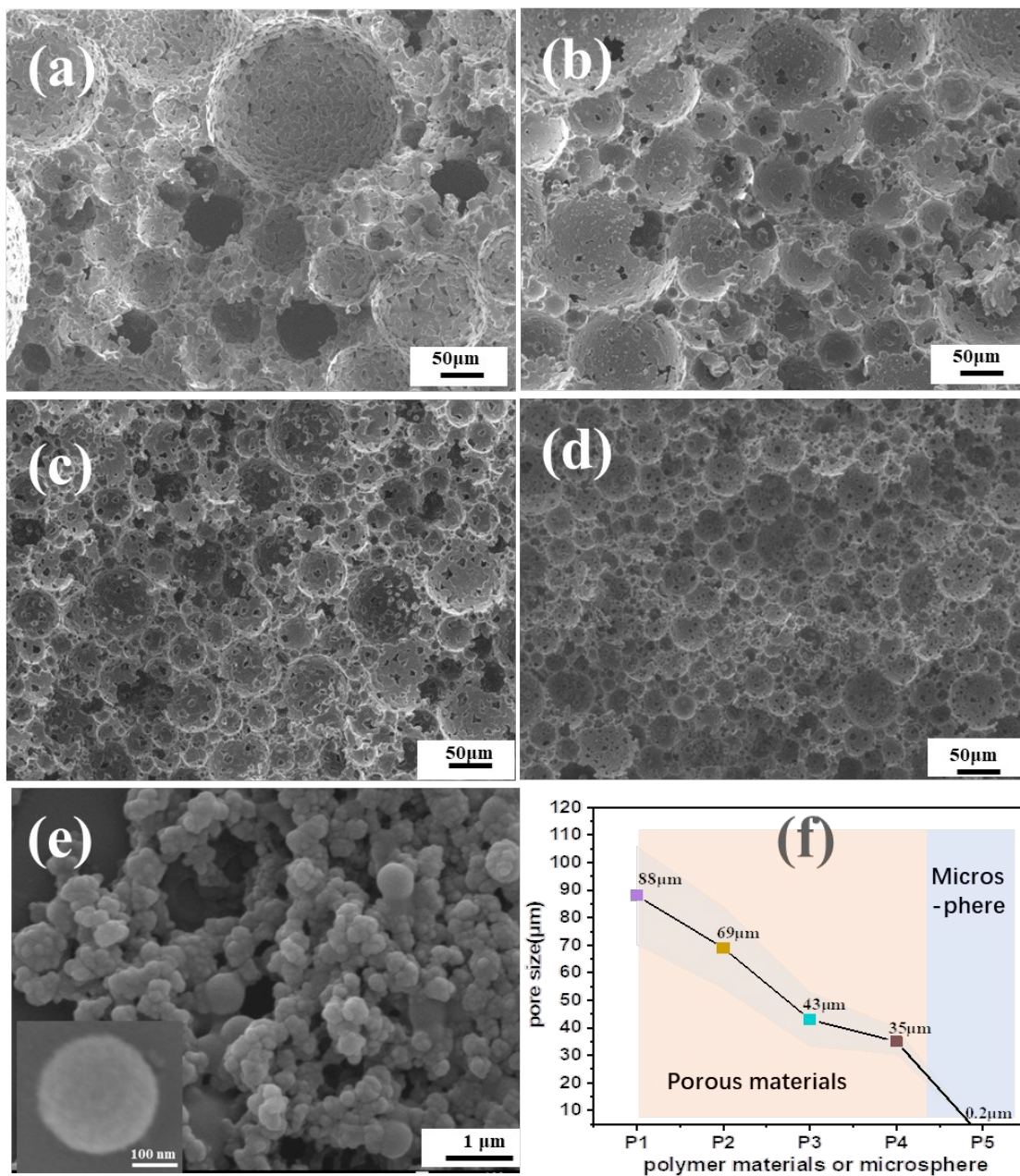


Figure 5. SEM of fluoro-porous materials stabilized by emulsifiers with different proportions of side groups from (a-e) referring to P1-P5. (f) Size distribution of porous and microsphere materials.

By varying the water/F-oil volume ratio from 1/1 to 3/1 with a 5 wt% P5 dissolved in the F-oil phase and water, an evolution of the emulsion from w/o to oil-in-water-in-oil (o/w/o), then to o/w is observed, as evidenced by the creaming/sedimentation of the dispersed phase and the fluorescent signals from the dispersed/continuous phases. (Figure 6a–c). Simultaneously, we can obtain porous materials, porous materials containing microspheres, and microsphere materials.

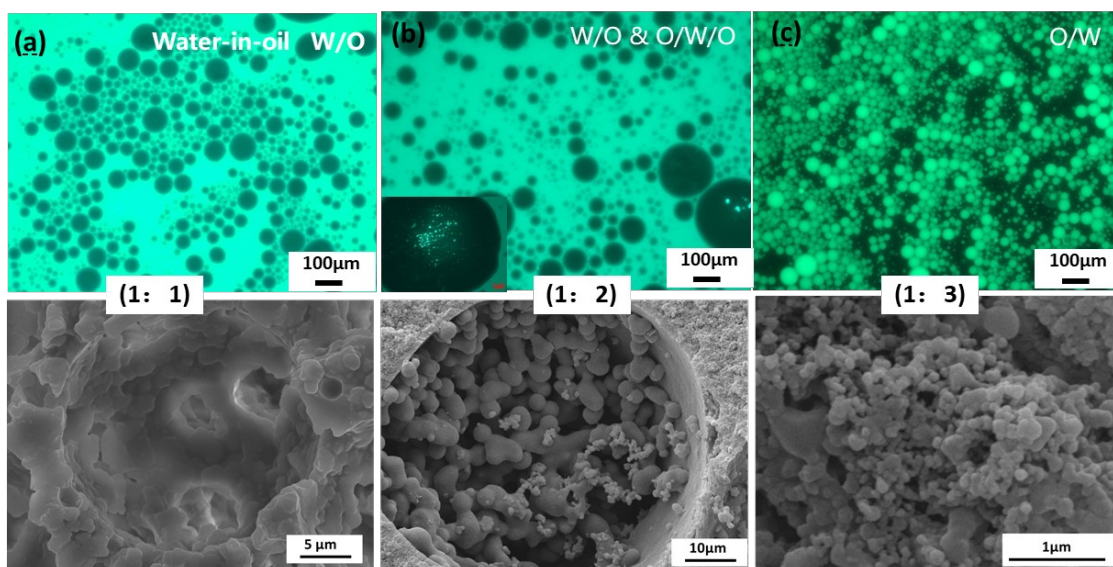


Figure 6. Fluorescent light microscope photograph and SEM of nanoparticles prepared from different emulsifier(P5) concentrations, (a) O:W=1:1, (b) O:W=1:2, (c) O:W=1:3; Oil phase was been dyed.

The surface wetting behavior of fluoro-polyHIPEs was investigated by measuring the contact angle of a pure water drop on the surface of fluoro-polyHIPEs. The measured value of 137.3° (Figure 7a) demonstrates the hydrophobic nature, due to the fluorine atoms contained within the materials (Figure 7b). When testing with oil droplets, oil phase droplets were adsorbed into the material almost instantaneously. The hydrophobic nature of the porous structure makes fluoro-

polyHIPEs promising candidates for absorbing organic solvents with different densities (Figure 7c). The adsorption capacities of fluoro-polyHIPEs for 8 different oils are shown in Figure 7d, and the highest adsorption capacity achieved for CHCl_3 is 630%. After adsorption, the oil could be desorbed by a simple centrifugation process, leaving the regeneration of fluoro-polyHIPE for a new absorption process. The cyclic adsorption/desorption of CHCl_3 was investigated. After five cycles, fluoro-polyHIPEs maintained essentially the same adsorption capacity, indicating the great potential of fluoro-polyHIPEs as reusable water–oil separation materials (Figure S9).

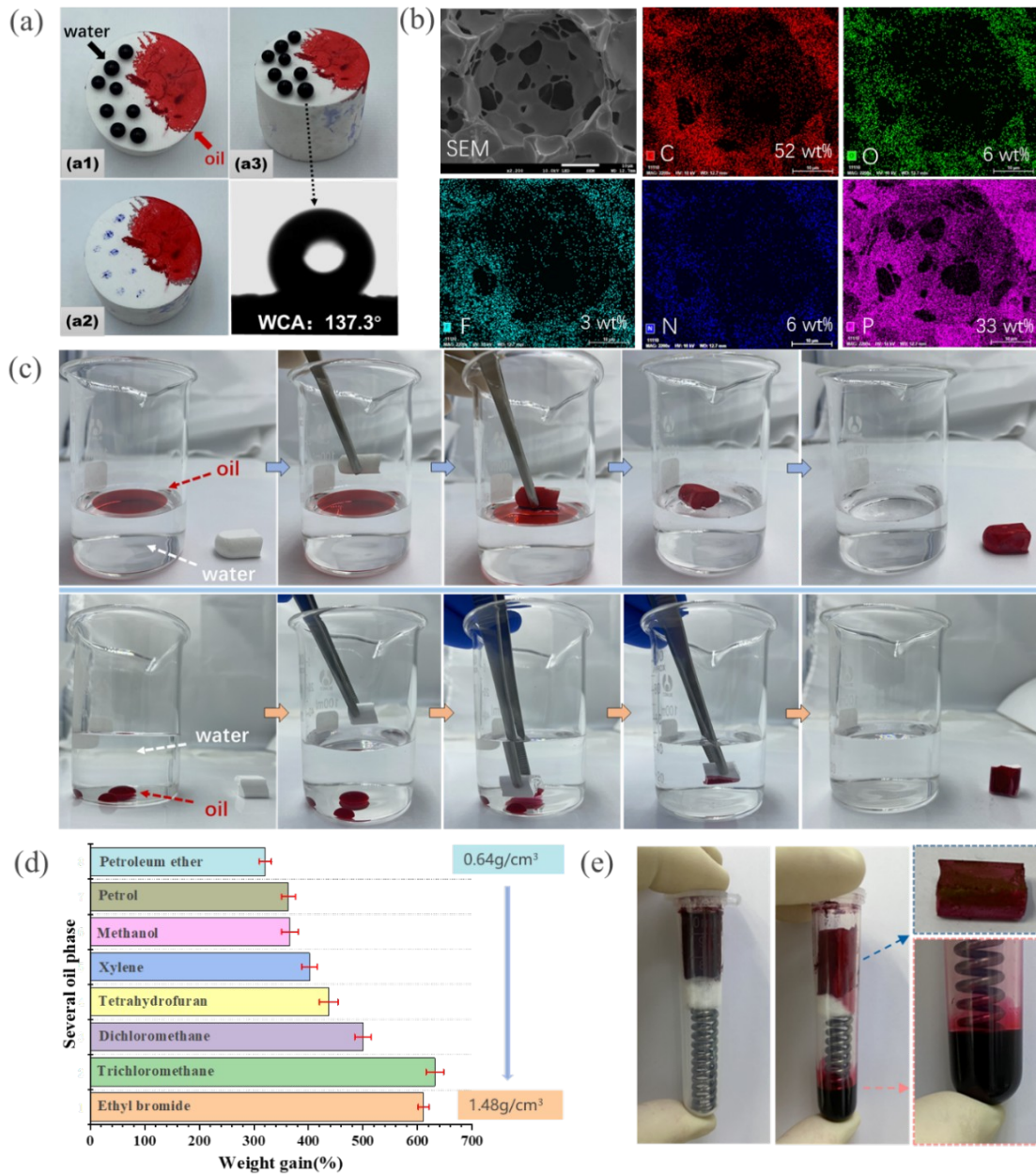


Figure 7. (a) Surface performance test of fluoro-porous material, (b) element distribution mapping diagram of porous material surface, (c) adsorption experiment of oil phase above and under water, (d) adsorption test of porous material for various organic oils of different densities, (e) centrifugal recovery of the adsorbed oil phase.

Conclusion

In this work, we reported the design and synthesis of amphiphilic PPZs for stabilizing fluoro-emulsions. The amphiphilic PPZs can be used as new macrosurfactants to stabilize fluoro-HIPE with different type of emulsion, including w/o and o/w emulsion. Furthermore, concentration and side group ratio of amphiphilic PPZ and volume ratio of water/F-oil had a significant impact on the morphology of the resulting materials. The resultant fluoropolymer foams show excellent adsorption performance towards several organic oils, due to the well-controlled porous structures. These significant properties of fluoropolymer foam will find promising applications in water/oil separations and porous templates for catalysts.

ASSOCIATED CONTENT

Supporting Information.

The Supporting Information is available free of charge on the ACS Publications website at DOI: XXXXXXXX.

Experimental section including materials, characterization, and additional experimental details (PDF).

AUTHOR INFORMATION

Corresponding Author

*E-mail: russell@mail.pse.umass.edu (T. P. Russell); shisw@mail.buct.edu.cn (S. Shi);

wuzp@mail.buct.edu.cn (Z. Wu:)

ORCID

T. P. Russell: 0000-0001-6384-5826

Shaowei Shi: 0000-0002-9869-4340

Zhanpeng Wu: 0000-0001-6605-0340

Notes

The authors declare no competing financial interest.

Funding Sources

This work was supported by Beijing Natural Science Foundation (2222071) and the National Natural Science Foundation of China (22372005, 52322310, 52173018, 51773010, 51873010)

REFERENCES

- (1) Alaimo, D.; Beigbeder, A.; Dubois, P.; Broze, G.; Jérôme, C.; Grignard, B., Block, Random and Palm-Tree Amphiphilic Fluorinated Copolymers: Controlled Synthesis, Surface Activity and Use as Dispersion Polymerization Stabilizers. *Polym. Chem.* **2014**, *5* (18), 5273-5282.
- (2) Zeng, X.; Ma, Y.; Wang, Y., Enhancing the Low Surface Energy Properties of Polymer Films with a Dangling Shell of Fluorinated Block-Copolymer. *Appl. Surf. Sci.* **2015**, *338*, 190-196.
- (3) Chen, X.; Zhou, J.; Ma, J., Synthesis of a Cationic Fluorinated Polyacrylate Emulsifier-Free Emulsion Via Ab Initio Raft Emulsion Polymerization and Its Hydrophobic Properties of Coating Films. *RSC Adv.* **2015**, *5* (118), 97231-97238.

- (4) Zhou, S.; Guan, J.; Li, Z.; Zhang, Q.; Zheng, J.; Li, S.; Zhang, S., Synthesis of Fluorinated Poly(Phenyl-Alkane)s of Intrinsic Microporosity by Regioselective Aldehyde (A2) + Aromatics (B2) Friedel–Crafts Polycondensation. *Macromolecules* **2021**, *54* (13), 6543-6551.
- (5) Wu, P.; Zhang, S.; Yang, H.; Zhu, Y.; Chen, J., Preparation of Emulsion-Templated Fluorinated Polymers and Their Application in Oil/Water Separation. *J. Polym. Sci., Part A: Polym. Chem.* **2018**, *56* (14), 1508-1515.
- (6) Tang, H.; Gou, Y.; Yan, Z.; Hu, Q.; Zhang, F.; Xiao, Q.; Zhong, Y.; Zhu, W., Copolymerization of 2-(Perfluorohexyl)Ethyl Methacrylate with Divinylbenzene to Fluorous Porous Polymeric Materials as Fluorophilic Absorbents. *Microporous Mesoporous Mater.* **2020**, *305*, 110398.
- (7) Ge, M.; Liu, H., Fluorine-Containing Silsesquioxane-Based Hybrid Porous Polymers Mediated by Bases and Their Use in Water Remediation. *Chem. - Eur. J.* **2018**, *24* (9), 2224-2231.
- (8) Lin, J.; Xia, X.; Liu, Y.; Luan, Z.; Chen, Y.; Ma, K.; Geng, B.; Li, H., Fabrication of Hierarchical Porous Fluoro-Polyhipe Materials with Ultra-High Specific Surface Area Via Hypercrosslinking Knitting Technique. *Journal of Applied Polymer Science* **2022**, *139* (38), e52914.
- (9) Zhou, T.; Moriyama, Y.; Ayukawa, Y.; Rakhmatia, Y. D.; Zhou, X.; Hu, J.; Koyano, K., Injectable Porous Bioresorbable Composite Containing Fluvastatin for Bone Augmentation. *ACS Biomater. Sci. Eng.* **2019**, *5* (10), 5422-5429.
- (10) Osman, S.; Senthil, R. A.; Pan, J.; Chai, L.; Sun, Y.; Wu, Y., Hierarchically Activated Porous Carbon Derived from Zinc-Based Fluorine Containing Metal-Organic Framework as

Extremely High Specific Capacitance and Rate Performance Electrode Material for Advanced Supercapacitors. *J. Colloid Interface Sci.* **2021**, *591*, 9-19.

(11) He, Q.; Jiang, J.; Zhu, J.; Pan, Z.; Li, C.; Yu, M.; Key, J.; Shen, P. K., A Facile and Cost Effective Synthesis of Nitrogen and Fluorine Co-Doped Porous Carbon for High Performance Sodium Ion Battery Anode Material. *J. Power Sources* **2020**, *448*, 227568.

(12) Azhar, U.; Huyan, C.; Wan, X.; Xu, A.; Li, H.; Geng, B.; Zhang, S., A Cationic Fluorosurfactant for Fabrication of High-Performance Fluoropolymer Foams with Controllable Morphology. *Mater. Des.* **2017**, *124*, 194-202.

(13) Dong, S.; Song, A.; Hao, J., Phase Behavior and $L\alpha$ -Phase of a New Catanionic System Formed by Cationic Hydrocarbon and Anionic Fluorocarbon Surfactants. *Colloids and Surfaces A: Physicochemical and Engineering Aspects* **2010**, *359* (1), 53-59.

(14) Wei, Z.; Chen, X.; Duan, J.; Zhan, G.; Wei, Y.; Zhang, A., Branched Chain Versus Straight Chain Fluorinated Surfactant: A Comparative Study of Their Anticorrosion Performance on Carbon Steel. *J. Mol. Liq.* **2019**, *280*, 327-333.

(15) Matusiak, J.; Grządka, E.; Kowalczyk, A.; Pietruszka, R.; Godlewski, M., The Influence of Hydrocarbon, Fluorinated and Silicone Surfactants on the Adsorption, Stability and Electrokinetic Properties of the K-Carrageenan/Alumina System. *J. Mol. Liq.* **2020**, *314*, 113669.

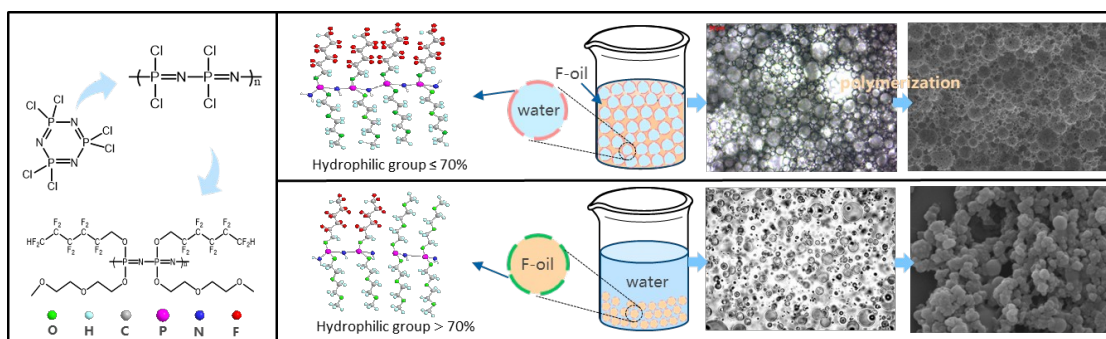
(16) Shrestha, L. K.; Sharma, S. C.; Sato, T.; Glatter, O.; Aramaki, K., Small-Angle X-Ray Scattering (Saxs) Study on Nonionic Fluorinated Micelles in Aqueous System. *J. Colloid Interface Sci.* **2007**, *316* (2), 815-824.

- (17) Mathieu, K.; Jérôme, C.; Debuigne, A., Influence of the Macromolecular Surfactant Features and Reactivity on Morphology and Surface Properties of Emulsion-Templated Porous Polymers. *Macromolecules* **2015**, *48* (18), 6489-6498.
- (18) Azhar, U.; Zong, C.; Wan, X.; Xu, A.; Yabin, Z.; Liu, J.; Zhang, S.; Geng, B., Methyl Methacrylate Hipe Solely Stabilized by Fluorinated Di-Block Copolymer for Fabrication of Highly Porous and Interconnected Polymer Monoliths. *Chem. - Eur. J.* **2018**, *24* (45), 11619-11626.
- (19) Wang, Y.; Wan, X.; He, J.; Azhar, U.; Chen, H.; Zhao, J.; Pang, A.-m.; Geng, B., A One-Step Fabrication and Modification of Hipe-Templated Fluoro-Porous Polymer Using Peg-B-Phfbma Macrosurfactant. *J. Mater. Sci.* **2020**, *55* (12), 4970-4986.
- (20) Wang, B.; Liu, T.; Chen, H.; Yin, B.; Zhang, Z.; Russell, T. P.; Shi, S., Molecular Brush Surfactants: Versatile Emulsifiers for Stabilizing and Structuring Liquids. **2021**, *60* (36), 19626-19630.
- (21) Wang, B.; Zhang, Z.; Feng, W.; Luo, J.; Shi, S., Stabilizing and Structuring Oil–Oil Interfaces by Molecular Brush Surfactants. **2022**, *3* (6), e292.
- (22) Chen, C.; Liu, X.; Tian, Z. C.; Allcock, H. R., Trichloroethoxy-Substituted Polyphosphazenes: Synthesis, Characterization, and Properties. *Macromolecules* **2012**, *45* (22), 9085-9091.
- (23) Allcock, H. R.; Kugel, R. L.; Valan, K. J., Phosponitrilic Compounds. Vi. High Molecular Weight Poly(Alkoxy- and Aryloxyphosphazenes). *Inorg. Chem.* **1966**, *5* (10), 1709-1715.

- (24) Zhang, S.; Ali, S.; Ma, H.; Zhang, L.; Wu, Z.; Wu, D.; Hu, T. S., Preparation of Poly(Bis(Phenoxy)Phosphazene) and ^{31}P Nmr Analysis of Its Structural Defects under Various Synthesis Conditions. *J. Phys. Chem. B* **2016**, *120* (43), 11307-11316.
- (25) Allcock, H. R.; Austin, P. E.; Neenan, T. X.; Sisko, J. T.; Blonsky, P. M.; Shriver, D. F., Polyphosphazenes with Etheric Side Groups: Prospective Biomedical and Solid Electrolyte Polymers. *Macromolecules* **1986**, *19* (6), 1508-1512.
- (26) Liao, Y.-F.; Zhou, M.-H.; Zhang, Y.; Peng, Y.-Y.; Jian, J.-X.; Lu, F.; Tong, Q.-X., Facile Synthesis and Marked Ph-Responsive Behavior of Novel Foaming Agents Based on Amide- and Ester-Linked Morpholine Fluorosurfactants. *J. Mol. Liq.* **2021**, *337*, 116577.
- (27) Peng, Y.-y.; Lu, F.; Tong, Q.-X., One-Step Synthesis, Wettability and Foaming Properties of High-Performance Non-Ionic Hydro-Fluorocarbon Hybrid Surfactants. *Appl. Surf. Sci.* **2018**, *433*, 264-270.
- (28) Chen, C.-L.; Liao, Y.-F.; Lu, F.; Zheng, Y.-S.; Peng, Y.-Y.; Ding, C.-W.; Tong, Q.-X., Facile Synthesis, Surface Activity, Wettability and Ultrahigh Foaming Properties of Novel Nonionic Gemini Fluorocarbon Surfactants. *J. Mol. Liq.* **2020**, *302*, 112469.
- (29) Abid, M. A.; Hussain, S.; Intisar, A.; Rizwan, M.; Ain, Q.; Mutahir, Z.; Yar, M.; Aamir, A.; Qureshi, A. K.; Jamil, M., Synthesis, Characterization, Hydrolytic Degradation, Mathematical Modeling and Antibacterial Activity of Poly[Bis((Methoxyethoxy)Ethoxy)Phosphazene] (Meep). *Polym. Bull.* **2021**, *78* (10), 6059-6072.

- (30) DeCollibus, D. P.; Marin, A.; Andrianov, A. K., Effect of Environmental Factors on Hydrolytic Degradation of Water-Soluble Polyphosphazene Polyelectrolyte in Aqueous Solutions. *Biomacromolecules* **2010**, *11* (8), 2033-2038.
- (31) Yu, T.; Swientoniewski, L. T.; Omarova, M.; Li, M.-C.; Negulescu, I. I.; Jiang, N.; Darvish, O. A.; Panchal, A.; Blake, D. A.; Wu, Q.; Lvov, Y. M.; John, V. T.; Zhang, D., Investigation of Amphiphilic Polypeptoid-Functionalized Halloysite Nanotubes as Emulsion Stabilizer for Oil Spill Remediation. *ACS Appl. Mater. Interfaces* **2019**, *11* (31), 27944-27953.
- (32) Fetsch, C.; Flecks, S.; Gieseler, D.; Marschelke, C.; Ulbricht, J.; van Pée, K.-H.; Luxenhofer, R., Self-Assembly of Amphiphilic Block Copolypeptoids with C2-C5 Side Chains in Aqueous Solution. *Macromolecular Chemistry and Physics* **2015**, *216* (5), 547-560.
- (33) Lau, T. H. M.; Wong, L. L. C.; Lee, K.-Y.; Bismarck, A., Tailored for Simplicity: Creating High Porosity, High Performance Bio-Based Macroporous Polymers from Foam Templates. *Green Chem.* **2014**, *16* (4), 1931-1940.
- (34) Qiao, Y.; Wang, X.; Zhang, X.; Xing, Z., Thermal Conductivity and Compressive Properties of Hollow Glass Microsphere Filled Epoxy–Matrix Composites. *J. Reinf. Plast. Compos.* **2015**, *34* (17), 1413-1421.
- (35) Zhan, H.-J.; Wu, K.-J.; Hu, Y.-L.; Liu, J.-W.; Li, H.; Guo, X.; Xu, J.; Yang, Y.; Yu, Z.-L.; Gao, H.-L.; Luo, X.-S.; Chen, J.-F.; Ni, Y.; Yu, S.-H., Biomimetic Carbon Tube Aerogel Enables Super-Elasticity and Thermal Insulation. *Chem* **2019**, *5* (7), 1871-1882.

For Table of Contents use only



We designed and prepared degradable amphiphilic polyphosphazenes to investigate the regulating effects on fluorinated emulsion. The regulatory mechanism of the amphiphilic polyphosphazenes at the interface between fluoro-oil and water was investigated. A simple change in the side group type of amphiphilic polyphosphazene can easily realize the transformation from water in oil emulsion to oil in water emulsion. The fluorinated materials obtained by emulsion polymerization showed good oil-water separation performance.

